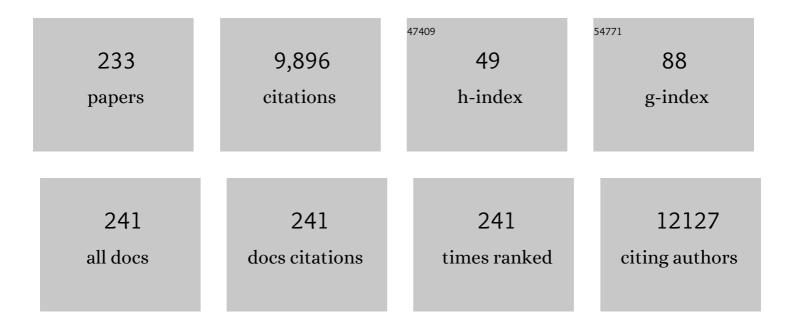
## Anders Wallqvist

List of Publications by Year in descending order

Source: https://exaly.com/author-pdf/7073622/publications.pdf Version: 2024-02-01



#	Article	IF	CITATIONS
1	Metabolic adjustments of blood-stage Plasmodium falciparum in response to sublethal pyrazoleamide exposure. Scientific Reports, 2022, 12, 1167.	1.6	8
2	Search for a Shared Genetic or Biochemical Basis for Biofilm Tolerance to Antibiotics across Bacterial Species. Antimicrobial Agents and Chemotherapy, 2022, , e0002122.	1.4	3
3	Metabolic changes accompanying the loss of fumarate hydratase and malate–quinone oxidoreductase in the asexual blood stage of Plasmodium falciparum. Journal of Biological Chemistry, 2022, 298, 101897.	1.6	7
4	Predicting changes in renal metabolism after compound exposure with a genome-scale metabolic model. Toxicology and Applied Pharmacology, 2021, 412, 115390.	1.3	10
5	TOXPANEL: A Gene-Set Analysis Tool to Assess Liver and Kidney Injuries. Frontiers in Pharmacology, 2021, 12, 601511.	1.6	5
6	Using the antibody-antigen binding interface to train image-based deep neural networks for antibody-epitope classification. PLoS Computational Biology, 2021, 17, e1008864.	1.5	19
7	Identifying functional metabolic shifts in heart failure with the integration of omics data and a heart-specific, genome-scale model. Cell Reports, 2021, 34, 108836.	2.9	15
8	Metabolic Survival Adaptations of Plasmodium falciparum Exposed to Sublethal Doses of Fosmidomycin. Antimicrobial Agents and Chemotherapy, 2021, 65, .	1.4	14
9	ToxProfiler: Toxicity-target profiler based on chemical similarity. Computational Toxicology, 2021, 18, 100162.	1.8	11
10	Immunoprofiling Correlates of Protection Against SHIV Infection in Adjuvanted HIV-1 Pox-Protein Vaccinated Rhesus Macaques. Frontiers in Immunology, 2021, 12, 625030.	2.2	6
11	Inter-study and time-dependent variability of metabolite abundance in cultured red blood cells. Malaria Journal, 2021, 20, 299.	0.8	7
12	Stochastic Model of the Adaptive Immune Response Predicts Disease Severity and Captures Enhanced Cross-Reactivity in Natural Dengue Infections. Frontiers in Immunology, 2021, 12, 696755.	2.2	4
13	Genomics and metabolomics of early-stage thioacetamide-induced liver injury: An interspecies study between guinea pig and rat. Toxicology and Applied Pharmacology, 2021, 430, 115713.	1.3	6
14	Obstructions in the lower airways lead to altered airflow patterns in the central airway. Respiratory Physiology and Neurobiology, 2020, 272, 103311.	0.7	8
15	Genome-Scale Model-Based Identification of Metabolite Indicators for Early Detection of Kidney Toxicity. Toxicological Sciences, 2020, 173, 293-312.	1.4	5
16	Toxicant-Induced Metabolic Alterations in Lipid and Amino Acid Pathways Are Predictive of Acute Liver Toxicity in Rats. International Journal of Molecular Sciences, 2020, 21, 8250.	1.8	8
17	Mechanism-based identification of plasma metabolites associated with liver toxicity. Toxicology, 2020, 441, 152493.	2.0	10
18	Concordance between Thioacetamide-Induced Liver Injury in Rat and Human In Vitro Gene Expression Data. International Iournal of Molecular Sciences, 2020, 21, 4017.	1.8	6

#	Article	IF	CITATIONS
19	A toxicogenomic approach to assess kidney injury induced by mercuric chloride in rats. Toxicology, 2020, 442, 152530.	2.0	8
20	Metabolic alterations in the erythrocyte during blood-stage development of the malaria parasite. Malaria Journal, 2020, 19, 94.	0.8	18
21	A mevalonate bypass system facilitates elucidation of plastid biology in malaria parasites. PLoS Pathogens, 2020, 16, e1008316.	2.1	30
22	A mevalonate bypass system facilitates elucidation of plastid biology in malaria parasites. , 2020, 16, e1008316.		0
23	A mevalonate bypass system facilitates elucidation of plastid biology in malaria parasites. , 2020, 16, e1008316.		Ο
24	A mevalonate bypass system facilitates elucidation of plastid biology in malaria parasites. , 2020, 16, e1008316.		0
25	A mevalonate bypass system facilitates elucidation of plastid biology in malaria parasites. , 2020, 16, e1008316.		Ο
26	Molecular Simulations Reveal the Role of Antibody Fine Specificity and Viral Maturation State on Antibody-Dependent Enhancement of Infection in Dengue Virus. Frontiers in Cellular and Infection Microbiology, 2019, 9, 200.	1.8	13
27	Volumetric characteristics of idiopathic pulmonary fibrosis lungs: computational analyses of high-resolution computed tomography images of lung lobes. Respiratory Research, 2019, 20, 216.	1.4	8
28	Assessing Chemical-Induced Liver Injury In Vivo From In Vitro Gene Expression Data in the Rat: The Case of Thioacetamide Toxicity. Frontiers in Genetics, 2019, 10, 1233.	1.1	14
29	Mining Public Toxicogenomic Data Reveals Insights and Challenges in Delineating Liver Steatosis Adverse Outcome Pathways. Frontiers in Genetics, 2019, 10, 1007.	1.1	14
30	Teaching an Old Dog New Tricks: Strategies That Improve Early Recognition in Similarity-Based Virtual Screening. Frontiers in Chemistry, 2019, 7, 701.	1.8	2
31	Conceptual Model of Biofilm Antibiotic Tolerance That Integrates Phenomena of Diffusion, Metabolism, Gene Expression, and Physiology. Journal of Bacteriology, 2019, 201, .	1.0	57
32	Genome-Scale Characterization of Toxicity-Induced Metabolic Alterations in Primary Hepatocytes. Toxicological Sciences, 2019, 172, 279-291.	1.4	15
33	Ten simple rules on how to create open access and reproducible molecular simulations of biological systems. PLoS Computational Biology, 2019, 15, e1006649.	1.5	25
34	Dynamics of the Tracheal Airway and Its Influences on Respiratory Airflows: An Exemplar Study. Journal of Biomechanical Engineering, 2019, 141, .	0.6	4
35	Short-term metabolic adjustments in Plasmodium falciparum counter hypoxanthine deprivation at the expense of long-term viability. Malaria Journal, 2019, 18, 86.	0.8	13
36	Network Modeling of Liver Metabolism to Predict Plasma Metabolite Changes During Short-Term Fasting in the Laboratory Rat. Frontiers in Physiology, 2019, 10, 161.	1.3	6

#	Article	IF	CITATIONS
37	Deep Neural Network Models for Predicting Chemically Induced Liver Toxicity Endpoints From Transcriptomic Responses. Frontiers in Pharmacology, 2019, 10, 42.	1.6	41
38	Mechanistic identification of biofluid metabolite changes as markers of acetaminophen-induced liver toxicity in rats. Toxicology and Applied Pharmacology, 2019, 372, 19-32.	1.3	32
39	A simplified metabolic network reconstruction to promote understanding and development of flux balance analysis tools. Computers in Biology and Medicine, 2019, 105, 64-71.	3.9	21
40	Molecular Similarity-Based Domain Applicability Metric Efficiently Identifies Out-of-Domain Compounds. Journal of Chemical Information and Modeling, 2019, 59, 181-189.	2.5	37
41	Dissecting Machine-Learning Prediction of Molecular Activity: Is an Applicability Domain Needed for Quantitative Structure–Activity Relationship Models Based on Deep Neural Networks?. Journal of Chemical Information and Modeling, 2019, 59, 117-126.	2.5	38
42	Genome-wide gene expression changes associated with exposure of rat liver, heart, and kidney cells to endosulfan. Toxicology in Vitro, 2018, 48, 244-254.	1.1	9
43	Comparative Proteomic Analysis of Liver Steatosis and Fibrosis after Oral Hepatotoxicant Administration in Sprague-Dawley Rats. Toxicologic Pathology, 2018, 46, 202-223.	0.9	14
44	Assessing Airflow Sensitivity to Healthy and Diseased Lung Conditions in a Computational Fluid Dynamics Model Validated In Vitro. Journal of Biomechanical Engineering, 2018, 140, .	0.6	26
45	Assessing Deep and Shallow Learning Methods for Quantitative Prediction of Acute Chemical Toxicity. Toxicological Sciences, 2018, 164, 512-526.	1.4	40
46	Identification of the Toxicity Pathways Associated With Thioacetamide-Induced Injuries in Rat Liver and Kidney. Frontiers in Pharmacology, 2018, 9, 1272.	1.6	35
47	General Approach to Estimate Error Bars for Quantitative Structure–Activity Relationship Predictions of Molecular Activity. Journal of Chemical Information and Modeling, 2018, 58, 1561-1575.	2.5	30
48	Metabolic network-based predictions of toxicant-induced metabolite changes in the laboratory rat. Scientific Reports, 2018, 8, 11678.	1.6	37
49	β-Aminoalcohols as Potential Reactivators of Aged Sarin-/Soman-Inhibited Acetylcholinesterase. ChemistrySelect, 2017, 2, 1885-1890.	0.7	5
50	Reconciled rat and human metabolic networks for comparative toxicogenomics and biomarker predictions. Nature Communications, 2017, 8, 14250.	5.8	151
51	Using a genome-scale metabolic network model to elucidate the mechanism of chloroquine action in Plasmodium falciparum. International Journal for Parasitology: Drugs and Drug Resistance, 2017, 7, 138-146.	1.4	26
52	Combinatorial peptide-based epitope mapping from Ebola virus DNA vaccines and infections reveals residue-level determinants of antibody binding. Human Vaccines and Immunotherapeutics, 2017, 13, 2953-2966.	1.4	4
53	Delayed fractional dose regimen of the RTS,S/AS01 malaria vaccine candidate enhances an IgG4 response that inhibits serum opsonophagocytosis. Scientific Reports, 2017, 7, 7998.	1.6	56
54	Molecular Structure-Based Large-Scale Prediction of Chemical-Induced Gene Expression Changes. Journal of Chemical Information and Modeling, 2017, 57, 2194-2202.	2.5	5

#	Article	IF	CITATIONS
55	Epitope mapping of Ebola virus dominant and subdominant glycoprotein epitopes facilitates construction of an epitope-based DNA vaccine able to focus the antibody response in mice. Human Vaccines and Immunotherapeutics, 2017, 13, 2883-2893.	1.4	10
56	Data-driven prediction of adverse drug reactions induced by drug-drug interactions. BMC Pharmacology & Toxicology, 2017, 18, 44.	1.0	35
57	vNN Web Server for ADMET Predictions. Frontiers in Pharmacology, 2017, 8, 889.	1.6	148
58	Quantitative Analysis of Repertoire-Scale Immunoglobulin Properties in Vaccine-Induced B-Cell Responses. Frontiers in Immunology, 2017, 8, 910.	2.2	8
59	Mechanisms of action of Coxiella burnetii effectors inferred from host-pathogen protein interactions. PLoS ONE, 2017, 12, e0188071.	1.1	12
60	Dengue virus antibody database: Systematically linking serotype-specificity with epitope mapping in dengue virus. PLoS Neglected Tropical Diseases, 2017, 11, e0005395.	1.3	19
61	A strategy for evaluating pathway analysis methods. BMC Bioinformatics, 2017, 18, 453.	1.2	27
62	Phenotypic Characterization of a Novel Virulence-Factor Deletion Strain of Burkholderia mallei That Provides Partial Protection against Inhalational Glanders in Mice. Frontiers in Cellular and Infection Microbiology, 2016, 6, 21.	1.8	13
63	Mining kidney toxicogenomic data by using gene co-expression modules. BMC Genomics, 2016, 17, 790.	1.2	44
64	Metabolic host responses to malarial infection during the intraerythrocytic developmental cycle. BMC Systems Biology, 2016, 10, 58.	3.0	20
65	The biological function of antibodies induced by the RTS,S/AS01 malaria vaccine candidate is determined by their fine specificity. Malaria Journal, 2016, 15, 301.	0.8	72
66	Using the Variable-Nearest Neighbor Method To Identify P-Glycoprotein Substrates and Inhibitors. ACS Omega, 2016, 1, 923-929.	1.6	7
67	General Purpose 2D and 3D Similarity Approach to Identify hERG Blockers. Journal of Chemical Information and Modeling, 2016, 56, 213-222.	2.5	20
68	Predicting Rat and Human Pregnane X Receptor Activators Using Bayesian Classification Models. Chemical Research in Toxicology, 2016, 29, 1729-1740.	1.7	21
69	Systems toxicology of chemically induced liver and kidney injuries: histopathologyâ€associated gene coâ€expression modules. Journal of Applied Toxicology, 2016, 36, 1137-1149.	1.4	27
70	Using Chemical-Induced Gene Expression in Cultured Human Cells to Predict Chemical Toxicity. Chemical Research in Toxicology, 2016, 29, 1883-1893.	1.7	7
71	Modeling the Role of Epitope Arrangement on Antibody Binding Stoichiometry in Flaviviruses. Biophysical Journal, 2016, 111, 1641-1654.	0.2	5
72	DBSecSys 2.0: a database of Burkholderia mallei and Burkholderia pseudomallei secretion systems. BMC Bioinformatics, 2016, 17, 387.	1.2	4

#	Article	IF	CITATIONS
73	Vinorelbine and epirubicin share common features with polysialic acid and modulate neuronal and glial functions. Journal of Neurochemistry, 2016, 136, 48-62.	2.1	10
74	Gene Expression Patterns Associated With Histopathology in Toxic Liver Fibrosis. Toxicological Sciences, 2016, 149, 67-88.	1.4	46
75	BRILIA: Integrated Tool for High-Throughput Annotation and Lineage Tree Assembly of B-Cell Repertoires. Frontiers in Immunology, 2016, 7, 681.	2.2	35
76	A systems biology strategy to identify molecular mechanisms of action and protein indicators of traumatic brain injury. Journal of Neuroscience Research, 2015, 93, 199-214.	1.3	14
77	Using host-pathogen protein interactions to identify and characterize Francisella tularensis virulence factors. BMC Genomics, 2015, 16, 1106.	1.2	33
78	A reverse-phase protein microarray-based screen identifies host signaling dynamics upon Burkholderia spp. infection. Frontiers in Microbiology, 2015, 6, 683.	1.5	11
79	Biofilm Formation Mechanisms of Pseudomonas aeruginosa Predicted via Genome-Scale Kinetic Models of Bacterial Metabolism. PLoS Computational Biology, 2015, 11, e1004452.	1.5	53
80	Neuroprotective mechanisms activated in non-seizing rats exposed to sarin. Brain Research, 2015, 1618, 136-148.	1.1	6
81	Mining Host-Pathogen Protein Interactions to Characterize Burkholderia mallei Infectivity Mechanisms. PLoS Computational Biology, 2015, 11, e1004088.	1.5	34
82	Critically Assessing the Predictive Power of QSAR Models for Human Liver Microsomal Stability. Journal of Chemical Information and Modeling, 2015, 55, 1566-1575.	2.5	28
83	Data-driven identification of structural alerts for mitigating the risk of drug-induced human liver injuries. Journal of Cheminformatics, 2015, 7, 4.	2.8	58
84	Structure-based pKa prediction provides a thermodynamic basis for the role of histidines in pH-induced conformational transitions in dengue virus. Biochemistry and Biophysics Reports, 2015, 4, 375-385.	0.7	13
85	Characterization of Chemically Induced Liver Injuries Using Gene Co-Expression Modules. PLoS ONE, 2014, 9, e107230.	1.1	45
86	Systems Level Analysis and Identification of Pathways and Networks Associated with Liver Fibrosis. PLoS ONE, 2014, 9, e112193.	1.1	71
87	Simulation of B Cell Affinity Maturation Explains Enhanced Antibody Cross-Reactivity Induced by the Polyvalent Malaria Vaccine AMA1. Journal of Immunology, 2014, 193, 2073-2086.	0.4	57
88	Tegaserod mimics the neurostimulatory glycan polysialic acid and promotes nervous system repair. Neuropharmacology, 2014, 79, 456-466.	2.0	26
89	Computational Approach To Characterize Causative Factors and Molecular Indicators of Chronic Wound Inflammation. Journal of Immunology, 2014, 192, 1824-1834.	0.4	56
90	Synthesis and evaluation of Strychnos alkaloids as MDR reversal agents for cancer cell eradication. Bioorganic and Medicinal Chemistry, 2014, 22, 1148-1155.	1.4	30

#	Article	IF	CITATIONS
91	Nonyloxytryptamine mimics polysialic acid and modulates neuronal and glial functions in cell culture. Journal of Neurochemistry, 2014, 128, 88-100.	2.1	25
92	A computational study of the respiratory airflow characteristics in normal and obstructed human airways. Computers in Biology and Medicine, 2014, 52, 130-143.	3.9	67
93	Modeling metabolism and stage-specific growth of Plasmodium falciparum HB3 during the intraerythrocytic developmental cycle. Molecular BioSystems, 2014, 10, 2526-2537.	2.9	16
94	A Reaction Path Study of the Catalysis and Inhibition of the <i>Bacillus anthracis</i> CapD γ-Glutamyl Transpeptidase. Biochemistry, 2014, 53, 6954-6967.	1.2	8
95	Exploiting large-scale drug-protein interaction information for computational drug repurposing. BMC Bioinformatics, 2014, 15, 210.	1.2	16
96	DBSecSys: a database of Burkholderia malleisecretion systems. BMC Bioinformatics, 2014, 15, 244.	1.2	9
97	Merging Applicability Domains for <i>in Silico</i> Assessment of Chemical Mutagenicity. Journal of Chemical Information and Modeling, 2014, 54, 793-800.	2.5	21
98	Prediction of Metabolic Flux Distribution from Gene Expression Data Based on the Flux Minimization Principle. PLoS ONE, 2014, 9, e112524.	1.1	43
99	Reconstituting protein interaction networks using parameter-dependent domain-domain interactions. BMC Bioinformatics, 2013, 14, 154.	1.2	17
100	3-Substituted Indole Inhibitors Against Francisella tularensis Fabl Identified by Structure-Based Virtual Screening. Journal of Medicinal Chemistry, 2013, 56, 5275-5287.	2.9	16
101	Bridging the gap between gene expression and metabolic phenotype via kinetic models. BMC Systems Biology, 2013, 7, 63.	3.0	19
102	Novel Burkholderia mallei Virulence Factors Linked to Specific Host-Pathogen Protein Interactions. Molecular and Cellular Proteomics, 2013, 12, 3036-3051.	2.5	38
103	A Fusion-Inhibiting Peptide against Rift Valley Fever Virus Inhibits Multiple, Diverse Viruses. PLoS Neglected Tropical Diseases, 2013, 7, e2430.	1.3	30
104	Exploring chemical reaction mechanisms through harmonic Fourier beads path optimization. Journal of Chemical Physics, 2013, 139, 165104.	1.2	3
105	Rapid Countermeasure Discovery against Francisella tularensis Based on a Metabolic Network Reconstruction. PLoS ONE, 2013, 8, e63369.	1.1	19
106	Computational and Experimental Validation of B and T-Cell Epitopes of the In Vivo Immune Response to a Novel Malarial Antigen. PLoS ONE, 2013, 8, e71610.	1.1	45
107	Identifying Cytochrome P450 Functional Networks and Their Allosteric Regulatory Elements. PLoS ONE, 2013, 8, e81980.	1.1	27
108	Modeling Phenotypic Metabolic Adaptations of Mycobacterium tuberculosis H37Rv under Hypoxia. PLoS Computational Biology, 2012, 8, e1002688.	1.5	65

#	Article	IF	CITATIONS
109	Efficient Conformational Sampling in Explicit Solvent Using a Hybrid Replica Exchange Molecular Dynamics Method. Journal of Chemical Theory and Computation, 2012, 8, 677-687.	2.3	24
110	Free Energy Difference in Indolicidin Attraction to Eukaryotic and Prokaryotic Model Cell Membranes. Journal of Physical Chemistry B, 2012, 116, 3387-3396.	1.2	16
111	Fungal bis-Naphthopyrones as Inhibitors of Botulinum Neurotoxin Serotype A. ACS Medicinal Chemistry Letters, 2012, 3, 387-391.	1.3	22
112	Probing the Donor and Acceptor Substrate Specificity of the $\hat{I}^3$ -Glutamyl Transpeptidase. Biochemistry, 2012, 51, 1199-1212.	1.2	44
113	QSAR Classification Model for Antibacterial Compounds and Its Use in Virtual Screening. Journal of Chemical Information and Modeling, 2012, 52, 2559-2569.	2.5	39
114	Locally Weighted Learning Methods for Predicting Dose-Dependent Toxicity with Application to the Human Maximum Recommended Daily Dose. Chemical Research in Toxicology, 2012, 25, 2216-2226.	1.7	27
115	Exploring Polypharmacology Using a ROCS-Based Target Fishing Approach. Journal of Chemical Information and Modeling, 2012, 52, 492-505.	2.5	78
116	Computational tools and resources for metabolism-related property predictions. 1. Overview of publicly available (free and commercial) databases and software. Future Medicinal Chemistry, 2012, 4, 1907-1932.	1.1	54
117	PathNet: a tool for pathway analysis using topological information. Source Code for Biology and Medicine, 2012, 7, 10.	1.7	67
118	2D SMARTCyp Reactivity-Based Site of Metabolism Prediction for Major Drug-Metabolizing Cytochrome P450 Enzymes. Journal of Chemical Information and Modeling, 2012, 52, 1698-1712.	2.5	30
119	Inferring high-confidence human protein-protein interactions. BMC Bioinformatics, 2012, 13, 79.	1.2	28
120	Classification of scaffold-hopping approaches. Drug Discovery Today, 2012, 17, 310-324.	3.2	275
121	A physicochemical descriptor-based scoring scheme for effective and rapid filtering of kinase-like chemical space. Journal of Cheminformatics, 2012, 4, 4.	2.8	18
122	Quantitative Predictions of Binding Free Energy Changes in Drug-Resistant Influenza Neuraminidase. PLoS Computational Biology, 2012, 8, e1002665.	1.5	16
123	Bioinformatic Analysis of Patient-Derived ASPS Gene Expressions and ASPL-TFE3 Fusion Transcript Levels Identify Potential Therapeutic Targets. PLoS ONE, 2012, 7, e48023.	1.1	22
124	Nonequilibrium Phase Transitions Associated with DNA Replication. Physical Review Letters, 2011, 106, 060601.	2.9	11
125	Spontaneous Buckling of Lipid Bilayer and Vesicle Budding Induced by Antimicrobial Peptide Magainin 2: A Coarse-Grained Simulation Study. Journal of Physical Chemistry B, 2011, 115, 8122-8129.	1.2	66
126	Molecular Dynamics Simulation of Solid-Supported Lipid Bilayers. Biophysical Journal, 2011, 100, 150a.	0.2	1

#	Article	IF	CITATIONS
127	Separation of Betti Reaction Product Enantiomers: Absolute Configuration and Inhibition of Botulinum Neurotoxin A. ACS Medicinal Chemistry Letters, 2011, 2, 396-401.	1.3	6
128	Modeling synergistic drug inhibition of Mycobacterium tuberculosis growth in murine macrophages. Molecular BioSystems, 2011, 7, 2622.	2.9	11
129	Improved Binding Free Energy Predictions from Single-Reference Thermodynamic Integration Augmented with Hamiltonian Replica Exchange. Journal of Chemical Theory and Computation, 2011, 7, 3001-3011.	2.3	41
130	Novel plant-derived recombinant human interferons with broad spectrum antiviral activity. Antiviral Research, 2011, 92, 461-469.	1.9	4
131	Categorizing Biases in High-Confidence High-Throughput Protein-Protein Interaction Data Sets. Molecular and Cellular Proteomics, 2011, 10, M111.012500.	2.5	25
132	On the proper calculation of electrostatic interactions in solid-supported bilayer systems. Journal of Chemical Physics, 2011, 134, 055109.	1.2	26
133	Can computationally designed protein sequences improve secondary structure prediction?. Protein Engineering, Design and Selection, 2011, 24, 455-461.	1.0	7
134	Accelerating Biomedical Research in Designing Diagnostic Assays, Drugs, and Vaccines. Computing in Science and Engineering, 2010, 12, 46-55.	1.2	3
135	Development and analysis of an in vivo-compatible metabolic network of Mycobacterium tuberculosis. BMC Systems Biology, 2010, 4, 160.	3.0	37
136	Unraveling the conundrum of seemingly discordant protein-protein interaction datasets. , 2010, 2010, 783-6.		12
137	An Integrated Docking Pipeline for the Prediction of Large-Scale Protein-Protein Interactions. , 2010, , .		0
138	Computing Relative Free Energies of Solvation Using Single Reference Thermodynamic Integration Augmented with Hamiltonian Replica Exchange. Journal of Chemical Theory and Computation, 2010, 6, 3427-3441.	2.3	23
139	A Novel Scoring Approach for Protein Co-Purification Data Reveals High Interaction Specificity. PLoS Computational Biology, 2009, 5, e1000515.	1.5	29
140	A systems biology framework for modeling metabolic enzyme inhibition of Mycobacterium tuberculosis. BMC Systems Biology, 2009, 3, 92.	3.0	34
141	<i>In silico</i> analyses of substrate interactions with human serum paraoxonase 1. Proteins: Structure, Function and Bioinformatics, 2009, 75, 486-498.	1.5	32
142	Structure and Dynamics of End-to-End Loop Formation of the Penta-Peptide Cys-Ala-Gly-Gln-Trp in Implicit Solvents. Journal of Physical Chemistry B, 2009, 113, 12382-12390.	1.2	19
143	Interaction of the Disordered Yersinia Effector Protein YopE with Its Cognate Chaperone SycE. Biochemistry, 2009, 48, 11158-11160.	1.2	6

144 A Web-Accessible Protein Structure Prediction Pipeline. , 2009, , .

0

#	Article	IF	CITATIONS
145	Influence of Protein Abundance on High-Throughput Protein-Protein Interaction Detection. PLoS ONE, 2009, 4, e5815.	1.1	39
146	PSPP: A Protein Structure Prediction Pipeline for Computing Clusters. PLoS ONE, 2009, 4, e6254.	1.1	13
147	DOVIS 2.0: an efficient and easy to use parallel virtual screening tool based on AutoDock 4.0. Chemistry Central Journal, 2008, 2, 18.	2.6	88
148	DOVIS: an implementation for high-throughput virtual screening using AutoDock. BMC Bioinformatics, 2008, 9, 126.	1.2	84
149	Evidence of probabilistic behaviour in protein interaction networks. BMC Systems Biology, 2008, 2, 11.	3.0	12
150	Free-Energy Profiles of Membrane Insertion of the M2 Transmembrane Peptide from Influenza A Virus. Biophysical Journal, 2008, 95, 5021-5029.	0.2	17
151	Membrane Insertion Profiles of Peptides Probed by Molecular Dynamics Simulations. , 2008, , .		Ο
152	Pharmacogenomics of the National Cancer Institute's 60-Tumor Cell Panel. , 2008, , 57-74.		0
153	FIEFDom: a transparent domain boundary recognition system using a fuzzy mean operator. Nucleic Acids Research, 2008, 37, 452-462.	6.5	27
154	Probing the Extent of Randomness in Protein Interaction Networks. PLoS Computational Biology, 2008, 4, e1000114.	1.5	13
155	DOVIS: A Tool for High-Throughput Virtual Screening. , 2007, , .		1
156	Anticancer medicines in development: assessment of bioactivity profiles within the National Cancer Institute anticancer screening data. Molecular Cancer Therapeutics, 2007, 6, 2261-2270.	1.9	45
157	Molecular Models of Water: Derivation and Description. Reviews in Computational Chemistry, 2007, , 183-247.	1.5	77
158	Chemoinformatic Analysis of NCI Preclinical Tumor Data:  Evaluating Compound Efficacy from Mouse Xenograft Data, NCI-60 Screening Data, and Compound Descriptors. Journal of Chemical Information and Modeling, 2007, 47, 1414-1427.	2.5	7
159	Assessment of in Vitro and in Vivo Activities in the National Cancer Institute's Anticancer Screen with Respect to Chemical Structure, Target Specificity, and Mechanism of Action. Journal of Medicinal Chemistry, 2006, 49, 1964-1979.	2.9	21
160	Evaluating Chemical Structure Similarity as an Indicator of Cellular Growth Inhibition. Journal of Chemical Information and Modeling, 2006, 46, 430-437.	2.5	20
161	Comprehensive analysis of pathway or functionally related gene expression in the National Cancer Institute's anticancer screen. Genomics, 2006, 87, 315-328.	1.3	42
162	Targeting changes in cancer: assessing pathway stability by comparing pathway gene expression coherence levels in tumor and normal tissues. Molecular Cancer Therapeutics, 2006, 5, 2417-2427.	1.9	15

#	Article	IF	CITATIONS
163	Differential Gene Expression as a Potential Classifier of 2-(4-Amino-3-methylphenyl)-5-fluorobenzothiazole-Sensitive and -Insensitive Cell Lines. Molecular Pharmacology, 2006, 69, 737-748.	1.0	5
164	Linking pathway gene expressions to the growth inhibition response from the National Cancer Institute's anticancer screen and drug mechanism of action. Pharmacogenomics Journal, 2005, 5, 381-399.	0.9	37
165	Anticancer metal compounds in NCI's tumor-screening database: putative mode of action. Biochemical Pharmacology, 2005, 69, 1009-1039.	2.0	158
166	Linking tumor cell cytotoxicity to mechanism of drug action: An integrated analysis of gene expression, small-molecule screening and structural databases. Proteins: Structure, Function and Bioinformatics, 2005, 59, 403-433.	1.5	39
167	Drugs aimed at targeting characteristic karyotypic phenotypes of cancer cells. Molecular Cancer Therapeutics, 2005, 4, 1559-1568.	1.9	16
168	Linking the growth inhibition response from the National Cancer Institute's anticancer screen to gene expression levels and other molecular target data. Bioinformatics, 2003, 19, 2212-2224.	1.8	29
169	Molecular classification of cancer: unsupervised self-organizing map analysis of gene expression microarray data. Molecular Cancer Therapeutics, 2003, 2, 317-32.	1.9	53
170	Mining the NCI screening database: explorations of agents involved in cell cycle regulation. Progress in Cell Cycle Research, 2003, 5, 173-9.	0.9	2
171	Detecting Native Protein Folds among Large Decoy Sets with the OPLS All-Atom Potential and the Surface Generalized Born Solvent Model. Advances in Chemical Physics, 2002, , 459-486.	0.3	2
172	Distinguishing native conformations of proteins from decoys with an effective free energy estimator based on the OPLS all-atom force field and the surface generalized born solvent model. Proteins: Structure, Function and Bioinformatics, 2002, 48, 404-422.	1.5	121
173	Fold Recognition using the OPLS All-Atom Potential and the Surface Generalized Born Solvent Model. Lecture Notes in Computational Science and Engineering, 2002, , 445-476.	0.1	0
174	Establishing connections between microarray expression data and chemotherapeutic cancer pharmacology. Molecular Cancer Therapeutics, 2002, 1, 311-20.	1.9	35
175	A Model for Studying Drying at Hydrophobic Interfaces: Structural and Thermodynamic Propertiesâ€. Journal of Physical Chemistry B, 2001, 105, 6745-6753.	1.2	98
176	Screening the molecular surface of human anticoagulant protein C: a search for interaction sites. Journal of Computer-Aided Molecular Design, 2001, 15, 13-27.	1.3	12
177	Simplified amino acid alphabets for protein fold recognition and implications for folding. Protein Engineering, Design and Selection, 2000, 13, 149-152.	1.0	207
178	Iterative sequence/secondary structure search for protein homologs: comparison with amino acid sequence alignments and application to fold recognition in genome databases. Bioinformatics, 2000, 16, 988-1002.	1.8	49
179	Cooperative Folding Units of Escherichia coli Tryptophan Repressor. Biophysical Journal, 1999, 77, 1619-1626.	0.2	4
180	Synthesis and Biological Properties of Novel Pyridinioalkanoyl Thiolesters (PATE) as Anti-HIV-1 Agents That Target the Viral Nucleocapsid Protein Zinc Fingers. Journal of Medicinal Chemistry, 1999, 42, 67-86.	2.9	112

#	Article	IF	CITATIONS
181	Structural analysis of inhibitor binding to HIV-1 protease: identification of a common binding motif. Computational and Theoretical Chemistry, 1998, 423, 93-100.	1.5	5
182	The C4b-binding protein–protein S interaction is hydrophobic in nature. BBA - Proteins and Proteomics, 1998, 1388, 181-189.	2.1	18
183	Structural investigation of C4b-binding protein by molecular modeling: Localization of putative binding sites. , 1998, 31, 391-405.		39
184	Hydrophobic Interactions in Aqueous Urea Solutions with Implications for the Mechanism of Protein Denaturation. Journal of the American Chemical Society, 1998, 120, 427-428.	6.6	290
185	Correlation between Native-State Hydrogen Exchange and Cooperative Residue Fluctuations from a Simple Model. Biochemistry, 1998, 37, 1067-1075.	1.2	162
186	A cooperative folding unit in HIV-1 protease. Implications for protein stability and occurrence of drug-induced mutations. Protein Engineering, Design and Selection, 1998, 11, 999-1005.	1.0	24
187	Topological Studies of the Amino Terminal Modules of Vitamin K-dependent Protein S Using Monoclonal Antibody Epitope Mapping and Molecular Modeling. Thrombosis and Haemostasis, 1998, 80, 798-804.	1.8	20
188	Topological studies of the amino terminal modules of vitamin K-dependent protein S using monoclonal antibody epitope mapping and molecular modeling. Thrombosis and Haemostasis, 1998, 80, 798-804.	1.8	4
189	Investigation of the temperature dependence of dielectric relaxation in liquid water by THz reflection spectroscopy and molecular dynamics simulation. Journal of Chemical Physics, 1997, 107, 5319-5331.	1.2	539
190	Analysis of protein-protein interactions and the effects of amino acid mutations on their energetics. The importance of water molecules in the binding epitope. Journal of Molecular Biology, 1997, 269, 281-297.	2.0	73
191	Azodicarbonamide inhibits HIV-1 replication by targeting the nucleocapsid protein. Nature Medicine, 1997, 3, 341-345.	15.2	107
192	Identification of cooperative folding units in a set of native proteins. Protein Science, 1997, 6, 1627-1642.	3.1	19
193	On the origins of the hydrophobic effect: observations from simulations of n-dodecane in model solvents. Biophysical Journal, 1996, 71, 600-608.	0.2	45
194	Atomic-scale analysis of the solvation thermodynamics of hydrophobic hydration. Biophysical Journal, 1996, 71, 1695-1706.	0.2	30
195	Evaluation of Selected Chemotypes in Coupled Cellular and Molecular Target-Based Screens Identifies Novel HIV-1 Zinc Finger Inhibitors. Journal of Medicinal Chemistry, 1996, 39, 3606-3616.	2.9	81
196	Docking enzymeâ€inhibitor complexes using a preferenceâ€based freeâ€energy surface. Proteins: Structure, Function and Bioinformatics, 1996, 25, 403-419.	1.5	53
197	The magnitude of the backbone conformational entropy change in protein folding. Proteins: Structure, Function and Bioinformatics, 1996, 25, 143-156.	1.5	222
198	A preference-based free-energy parameterization of enzyme-inhibitor binding. Applications to HIV-1-protease inhibitor design. Protein Science, 1995, 4, 1881-1903.	3.1	131

#	Article	IF	CITATIONS
199	Liquid densities and structural properties of molecular models of water. Journal of Chemical Physics, 1995, 102, 6559-6565.	1.2	41
200	Molecular Dynamics Study of the Dependence of Water Solvation Free Energy on Solute Curvature and Surface Area. The Journal of Physical Chemistry, 1995, 99, 2885-2892.	2.9	140
201	Free-Energy Cost of Bending n-Dodecane in Aqueous Solution. Influence of the Hydrophobic Effect and Solvent Exposed Area. The Journal of Physical Chemistry, 1995, 99, 13118-13125.	2.9	31
202	Cooperativity of Water-Solute Interactions at a Hydrophilic Surface. The Journal of Physical Chemistry, 1995, 99, 5705-5712.	2.9	4
203	Computer Simulation of Hydrophobic Hydration Forces on Stacked Plates at Short Range. The Journal of Physical Chemistry, 1995, 99, 2893-2899.	2.9	279
204	Molecular Dynamics Simulations of 2 m Aqueous Urea Solutions. The Journal of Physical Chemistry, 1994, 98, 8224-8233.	2.9	62
205	Nonempirical intermolecular potentials for urea–water systems. Journal of Chemical Physics, 1994, 100, 1262-1273.	1.2	79
206	A simplified amino acid potential for use in structure predictions of proteins. Proteins: Structure, Function and Bioinformatics, 1994, 18, 267-280.	1.5	74
207	Discussion of "Water and Aqueous Solutions Near Freezing". Annals of the New York Academy of Sciences, 1994, 715, 159-160.	1.8	0
208	Computer Simulations of Type I Gas Hydrates in the Presence of Methanol. Annals of the New York Academy of Sciences, 1994, 715, 540-542.	1.8	2
209	Effective potentials for liquid water using polarizable and nonpolarizable models. The Journal of Physical Chemistry, 1993, 97, 13841-13851.	2.9	140
210	On the Implementation of Friedman Boundary Conditions in Liquid Water Simulations. Molecular Simulation, 1993, 10, 13-17.	0.9	27
211	On the stability of type I gas hydrates in the presence of methanol. Journal of Chemical Physics, 1992, 96, 5377-5382.	1.2	30
212	Pressure dependence of methane solvation in aqueous mixtures and the relation to the structure of liquid water. Journal of Chemical Physics, 1992, 96, 1655-1656.	1.2	26
213	Properties of urea–water solvation calculated from a newabinitiopolarizable intermolecular potential. Journal of Chemical Physics, 1991, 95, 8419-8429.	1.2	70
214	New intermolecular energy calculation scheme: applications to potential surface and liquid properties of water [Erratum to document cited in CA112(12):105129h]. The Journal of Physical Chemistry, 1991, 95, 4922-4922.	2.9	12
215	Molecular dynamics study of hydrophobic aggregation in water/methane/methanol systems. Chemical Physics Letters, 1991, 182, 237-241.	1.2	29
216	Properties of flexible water models. Molecular Physics, 1991, 74, 515-533.	0.8	146

#	Article	IF	CITATIONS
217	Intermolecular Potential Variation due to Intramolecular Rotation in Molecules. Molecular Simulation, 1991, 7, 195-204.	0.9	1
218	On the basis set superposition error in the evaluation of water dimer interactions. The Journal of Physical Chemistry, 1991, 95, 6395-6396.	2.9	17
219	Molecular dynamics study of a hydrophobic aggregate in an aqueous solution of methane. The Journal of Physical Chemistry, 1991, 95, 8921-8927.	2.9	65
220	Intermolecular interactions of urea and water. Journal De Chimie Physique Et De Physico-Chimie Biologique, 1991, 88, 2457-2464.	0.2	8
221	New intermolecular energy calculation scheme: applications to potential surface and liquid properties of water. The Journal of Physical Chemistry, 1990, 94, 1649-1656.	2.9	154
222	Ewald summation retards translational motion in molecular dynamics simulation of water. International Journal of Quantum Chemistry, 1990, 38, 245-249.	1.0	7
223	Polarizable water at a hydrophobic wall. Chemical Physics Letters, 1990, 165, 437-442.	1.2	73
224	Incorporating intramolecular degrees of freedom in simulations of polarizable liquid water. Chemical Physics, 1990, 148, 439-449.	0.9	48
225	A molecular dynamics study of polarizable water. Molecular Physics, 1989, 68, 563-581.	0.8	407
226	Hydrophobic interaction between a methane molecule and a paraffin wall in liquid water. Chemical Physics Letters, 1988, 145, 26-32.	1.2	38
227	Comment on: a€ a€ Watera€ water and watera€ ion potential functions including terms for manya€oody effects,'' T. P. Lybrand and P. Kollman, J. Chem. Phys. 83, 2923 (1985), and on 'â€`Calculation of free er changes in ionâ€`water clusters using nonadditive potentials and the Monte Carlo method,'' P. Cieplak, T. P. Lybrand, and P. Kollman, J. Chem. Phys. 86, 6393 (1987). Journal of Chemical Physics, 1988, 88,	nergy 1.2	8
228	Behavior of the hydrated electron at different temperatures: structure and absorption spectrum. The Journal of Physical Chemistry, 1988, 92, 1721-1730.	2.9	110
229	Path integral Monte Carlo study of the hydrated electron. Journal of Chemical Physics, 1987, 86, 6404-6418.	1.2	116
230	Path-integral Monte Carlo simulations of electron localization in water clusters. Journal of Statistical Physics, 1986, 43, 973-984.	0.5	11
231	Localization of an excess electron in water clusters. Journal of Chemical Physics, 1986, 85, 1583-1591.	1.2	120
232	Path-integral simulation of pure water. Chemical Physics Letters, 1985, 117, 214-219.	1.2	106
233	Intermolecular potentials for the water-benzene and the benzene-benzene systems calculated in an ab initio SCFCI approximation. Journal of the American Chemical Society, 1983, 105, 3777-3782.	6.6	303